Published in final edited form as:
Biomaterials. 2012 January ; 33(1): 80–90. doi:10.1016/j.biomaterials.2011.09.041.

Enhancement of mesenchymal stem cell angiogenic capacity and stemness by a biomimetic hydrogel scaffold

Kristine C. Rustad[a], **Victor W. Wong**[a], **Michael Sorkin**[a], **Jason P. Glotzbach**[a], **Melanie R. Major**[a], **Jayakumar Rajadas**[b], **Michael T. Longaker**[a], and **Geoffrey C. Gurtner**[a,*]

[a]Department of Surgery, Stanford University, 257 Campus Drive, GK 201, Stanford, CA 94305, USA

[b]Biomaterials and Advanced Drug Delivery Service Center, Stanford, CA, USA

Abstract

In this study, we examined the capacity of a biomimetic pullulan–collagen hydrogel to create a functional biomaterial-based stem cell niche for the delivery of mesenchymal stem cells (MSCs) into wounds. Murine bone marrow-derived MSCs were seeded into hydrogels and compared to MSCs grown in standard culture conditions. Hydrogels induced MSC secretion of angiogenic cytokines and expression of transcription factors associated with maintenance of pluripotency and self-renewal (Oct4, Sox2, Klf4) when compared to MSCs grown in standard conditions. An excisonal wound healing model was used to compare the ability of MSC-hydrogel constructs versus MSC injection alone to accelerate wound healing. Injection of MSCs did not significantly improve time to wound closure. In contrast, wounds treated with MSC-seeded hydrogels showed significantly accelerated healing and a return of skin appendages. Bioluminescence imaging and FACS analysis of luciferase+/GFP+ MSCs indicated that stem cells delivered within the hydrogel remained viable longer and demonstrated enhanced engraftment efficiency than those delivered via injection. Engrafted MSCs were found to differentiate into fibroblasts, pericytes and endothelial cells but did not contribute to the epidermis. Wounds treated with MSC-seeded hydrogels demonstrated significantly enhanced angiogenesis, which was associated with increased levels of VEGF and other angiogenic cytokines within the wounds. Our data suggest that biomimetic hydrogels provide a functional niche capable of augmenting MSC regenerative potential and enhancing wound healing.

Keywords

Mesenchymal stem cell; Hydrogel; Wound healing; Growth factors

1. Introduction

Mesenchymal stem cells (MSCs) have shown beneficial effects in preclinical models of wound healing and in preliminary clinical case reports by accelerating wound closure,

* Corresponding author. Tel.: +1 650 724 6672; fax: +1 650 724 9501. ggurtner@stanford.edu (G.C. Gurtner)..

improving neovascularization, and reducing scar formation [1-6]. While the specific mechanism for MSC-mediated improvements in wound healing has not been fully elucidated, a significant role for paracrine interactions in this process has been proposed [7,8]. The role of MSC differentiation into different cell types within the wound environment has been less well established partially due to the small number of transplanted cells that persist within the wound over time. The lack of significant MSC engraftment at sites of injury is thought to be a major limiting factor of current MSC-based therapeutics [9].

The problem of low MSC engraftment is not unique to wounds and has plagued the therapeutic application of MSCs in numerous models of tissue injury. Despite variable degrees of enhanced tissue repair, MSCs administered systemically have shown long-term engraftment rates of less than 3% in injury models of the pancreas [10], heart [11], kidney [12] and liver [13]. Delivery of MSCs via local injection to cutaneous wound sites has similarly demonstrated low engraftment efficiency [1]. The capacity of MSC-based treatments to exhibit therapeutic efficacy despite such low engraftment efficiency has spurred efforts to improve cell delivery methods in hope of maximizing the regenerative potential of MSCs.

The use of collagen matrices to deliver MSCs in animal models of myocardial infarction has shown promise in augmenting cell engraftment and improving functional endpoints [14,15]. Similarly, an injectable collagen-based matrix was used to successfully increase the engraftment efficiency of endothelial progenitor cells and upregulate local angiogenesis in a rodent hindlimb ischemia model [16]. These and other tissue engineering-based strategies have suggested that the use of biomaterial-based scaffolds for cell delivery may not only enhance cell viability but can also promote cell proliferation and actively contribute to MSC fate determination [17].

We and others have previously proposed that the ultimate solution to pathologic healing is delivery of multipotent cells in the context of appropriate environmental cues [18,19]. The use of acellular dermal matrices for stem cell delivery into wounds has shown promise in directing skin-specific regeneration [20]. However, the problems associated with natural biomaterials including cost, availability, seeding and the theoretical risk of disease transmission prompted us to examine synthetic biomaterials that could recapitulate the beneficial structural, mechanical and chemical properties of skin without these problems.

Hydrogels are an ideal physicochemical mimetic of natural extracellular matrix (ECM) as the hygroscopic nature of ECM is one of its key properties [21]. Additionally, a wide array of commercially available hydrogel products are already used for wound dressings, thus potentially accelerating the translation of this technology into the clinic. In this study, we utilize a biomimetic hydrogel scaffold previously developed by our laboratory to deliver MSCs into wounds within a three-dimensional dermal-like microenvironment. We have previously demonstrated that this composite collagen-pullulan hydrogel is non-cytotoxic, recapitulates key features of fetal (scarless) healing, and promotes granulation tissue formation through vascular induction [22]. This cell-biomimetic matrix approach for stem cell delivery may be a promising clinical strategy for maximizing the therapeutic potential of MSCs for cutaneous wound healing.

2. Materials and methods

2.1. Animals

All mice were housed in the Stanford University Veterinary Service Center in accordance with NIH and institution-approved animal care guidelines. All procedures were approved by the Stanford Administrative Panel on Laboratory Animal Care.

2.2. Bone marrow-derived MSC isolation

Luciferase+/GFP+ bone marrow-derived MSCs were isolated as previously described [23]. Briefly, bone marrow was flushed from the tibias and femurs of 8–12 week old male FVB-luc-eGFP transgenic mice (generous gift of Dr. Christopher Contag) into a suspension of 1% fetal bovine serum (FBS, Invitrogen, Carlsbad, CA) in phosphate buffered saline (PBS, Invitrogen). Cells were then passed through a 100 μm filter and plated on plastic tissue culture dishes in Dulbecco's Modified Eagle's Medium (DMEM, Invitrogen) supplemented with 10% FBS and 1% penicillin-streptomycin (Invitrogen). Media was changed 48 h after initial plating to remove all non-adherent cells, and MSCs were selected out by plastic adherence. Cells were used at passages 3 to 6 for all experiments.

2.3. Hydrogel fabrication

Collagen-pullulan hydrogels were fabricated as previously described [22]. Briefly, a composite mixture of 2 g pullulan (Hayashibara Laboratories, Okayama, Japan), 2 g sodium trimetaphosphate (Sigma–Aldrich) and 2 g KCl (Sigma–Aldrich) in H_2O was mixed with 5% (w/w) rat tail collagen I (Sigma–Aldrich). The mixture was poured onto sheets and compressed to create 2 mm-thick films. Films were dehydrated in 100% ethyl alcohol and dried for 12 h. Dried films were washed in PBS until a wash pH of 7.0 was reached.

2.4. Cell seeding and in vitro analyses

Single cell suspensions of 2.5×10^5 MSCs in 100 μL of media were added dropwise to pre-cut 6 mm hydrogel scaffolds and incubated at 37 °C in 5% CO_2. Imaging of MSCs seeded on scaffolds with variable pressure SEM was performed as previously described [22]. A live/dead assay was used to assess cell viability of MSCs seeded within hydrogels for 1, 3, 7 or 14 days per manufacturer's instructions (Live/Dead Double Staining Kit, Calbiochem, Gibbstown, NJ). Images were obtained with fluorescence microscopy (Zeiss Axioplan 2 Imaging, Carl Zeiss, Inc., Thornwood, NY) with band-pass filters set to detect FITC and Texas Red.

To assess the capacity of MSCs to migrate through the hydrogel matrix, a transwell migration assay was performed using the 8.0 μm HTS Transwell-96 permeable support (Corning Life Sciences – Axygen, Inc., Union City, CA) and mouse PDGF-BB (10 ng/mL, Abcam Inc., Cambridge, MA) as the chemotactic stimulant ($n = 6$). Hydrogel scaffolds were placed within the top chamber of the transwell support so that the permeable membrane separating the two chambers was completely covered by the hydrogel matrix. Twenty-four hours after MSC seeding, membranes were removed and fixed in 4% paraformaldehyde. Cell nuclei were stained with Vectashield Mounting Medium with DAPI (Vector Laboratories, Burlingame, CA).

An MTT assay was used to assess MSC proliferation as described previously [24].

2.5. Real-time quantitative PCR analysis

MSCs were seeded into scaffolds or plated into each well of a 6-well plate and incubated at 37 °C in 5% CO_2 for 24 h (n = 7). Total RNA was harvested from MSCs within scaffolds as described previously [25] (RNeasy Plant Mini kit, Quiagen, Germantown, MD) and from plated MSC cultures (RNeasy Mini kit, Qiagen). Extracted RNA underwent reverse transcription (Superscript First-Strand Synthesis kit, Invitrogen) and real-time qPCR reactions were performed using 2× Universal Taqman PCR Master Mix (Applied Biosystems, Foster City, CA) and Taqman gene expression assays for *Pou5f1* (Oct4, Mm00658129_g1), *Sox2* (Mm00488369_s1), *Klf4* (Kruppel-like growth factor 4, Mm00516104_m1), *Vegf-a* (Vascular endothelial growth factor-A, Mm01281447_m1), *Ccl2* (Monocyte chemoattractant protein-1/Mcp-1, Mm00441242_m1), *Fgf-1* (Fibroblast growth factor-1, Mm00438906_m1), *Cxcl12* (Stromal cell-derived factor-1/Sdf-1, Mm00445553_m1), *Angpt2* (Angiopoietin 2, Mm00545822_m1), *Hgf* (Hepatocyte growth factor, Mm01135193_m1), *Angpt1* (Angiopoietin 1, Mm00456503_m1), *Igf-1* (Insulin-like growth factor-1, Mm00439560_m1), and *Fgf-2* (Fibroblast growth factor-2, Mm00433287_m1) using a Prism 7900HT Sequence Detection System (Applied Biosystems, Carlsbad, CA). Levels of *Actb* (Beta actin, Mm01205647_g1) were quantified in parallel as an internal control, and gene expression was normalized accordingly.

2.6. Western blotting

Total protein was isolated from MSCs seeded onto hydrogels or plated for 24 h (n = 4) and separated on a 4–12% polyacrylamide gel (Invitrogen) followed by transfer to a nitrocellulose membrane (Invitrogen). Anti-Oct4 (1:800), anti-Sox2 (1:1000) anti-Klf4 (1:700) and anti-β-actin (1:3000) were used as primary antibodies. An HRP-conjugated secondary antibody was used (1:10,000) and detected using the ECL Plus Western Blotting Detection Kit (GE Healthcare, Waukesha, WI). All antibodies were purchased from Abcam Inc.

2.7. Immunofluorescence

MSCs seeded onto coverslips or onto pre-cut 6 mm hydrogel scaffolds for 24 h were fixed in 4% paraformaldehyde for 1.5 h then incubated with primary antibodies against Oct4 (1:200), Sox2 (1:500) or Klf4 (1:500) followed by AlexaFluor 594-conjugated secondary antibody (Invitrogen). Cell nuclei were stained with DAPI.

2.8. ELISA

Conditioned media was collected from MSCs seeded onto hydrogels or plated in wells of a 96-well plate after 24 h (n = 8). Protein levels of VEGF-A and MCP-1 were quantified using the mouse Quantikine ELISA Kit (R&D Systems, Minneapolis, MN).

2.9. Excisional wound healing model

Eight to twelve-week old female C57Bl/6 mice (Jackson Laboratories, Bar Harbor, ME) were randomized to four treatment groups: no treatment, hydrogel alone, local MSC

injection, or MSC-seeded hydrogel treatment (n = 12 wounds per treatment group). A stented excisional wound healing model was used as previously published [26]. Briefly, after induction of anesthesia, the dorsal surface of the mouse was shaved and depilated. Two 6 mm full thickness wounds were created on either side of the midline. Wounds were circumscribed by donut-shaped silicone splints held in place using 6-0 nylon sutures to prevent wound contraction. For the MSC injection group, 2.5×10^5 luc+/GFP + MSCs suspended in 80 μL of PBS were injected subcutaneously at four equidistant points around the wound edge. For the hydrogel alone and MSC-seeded hydrogel groups, hydrogel scaffolds that were either unseeded or seeded with 2.5×10^5 luc+/GFP + MSCs 24 h prior to wounding were washed in sterile PBS three times prior to being placed within each wound. All wounds were covered with an occlusive dressing (Tegaderm, 3M, St. Paul, MN). Digital photographs were taken at days 0, 1 and every other day after, and wound area was measured using Image J software (NIH, Bethesda, MD). Percent of original wound area was defined as: (wound area on day 1 – wound area day "X")/(wound area on day 1) × 100. Wound closure was determined through assessment of digital wound images by three blinded evaluators.

2.10. In vivo bioluminescence imaging

Bioluminescence imaging was used to assess viability of delivered MSCs in vivo. Mice treated with subcutaneous MSC injection or MSC-seeded hydrogels (n = 14) were injected intraperitoneally with 150 mg/kg D-luciferin (Biosynth International, Inc., Itasca, IL) in PBS. Mice were anesthetized and images were obtained after 10 min with a cooled CCD camera using the Xenogen IVIS 200 System (Caliper Life Sciences, Mountain View, CA). Bioluminescence of a set region of interest centered on each wound was subtracted from background luminescence and quantified as units of total flux (photons per second) using Living Image Software (version 3.2, Caliper Life Sciences).

2.11. Histologic analysis

Wounds were harvested and immediately embedded in OCT (Sakura Finetek USA, Inc., Torrance, CA) or fixed in 4% paraformaldehyde overnight and embedded in paraffin. For histologic localization of GFP + cells, paraffin sections were cleared in xylenes for 10 min then rehydrated and stained with DAPI. Paraffin sections were stained with hematoxylin and eosin (H&E, Sigma–Aldrich). Seven micron-thick frozen sections were fixed in acetone at −20 °C twice for 10 min and immunostained using antibodies against Hsp47 (1:1000), cytokeratin 5 (1:300), NG2 (1:100), or CD31 (1:200, BD Biosciences). GFP + MSCs were labeled with FITC-conjugated antibody against GFP (1:100). All antibodies were purchased from Abcam Inc. unless otherwise indicated. For dermal microvessel counts, luminal structures containing red blood cells were considered microvessels. For each condition, four high power fields at 400× were examined for three separate wound samples by three independent blinded observers. Frozen sections were stained to assess wound vasculature with a phycoerythrin-conjugated antibody to CD31 (1:100, Abcam). Nuclei were stained with DAPI. ImageJ was used to binarize immunofluorescent images taken with the same excitation, gain and exposure settings as previously described [27]. Intensity threshold values were set automatically and quantification of CD31 staining was determined by pixel-positive area normalized to dermal area.

2.12. Flow cytometry

For quantification of GFP + MSC engraftment in wounded skin, four to six wounds and 2 mm of surrounding skin were excised at day 7, 14 and 28 post-wounding. Tissue was minced and incubated in 0.5 mg/mL Liberase TL (Roche Applied Science, Indianapolis, IN) for 1 h at 37 °C. Appropriate isotype controls, unstained cells, and untreated wounds were used as controls. Flow cytometry was performed on a BD FACSAria cell sorter (BD Biosciences) and subsequently analyzed using FlowJo digital FACS software (Tree Star, Inc., Ashland, OR). Aggregated cells were excluded, and background autofluorescence in untreated wounds was subtracted from each treated sample to determine the percentage of GFP + cells in wounds.

2.13. Wound angiogenic cytokine quantification

Wounds were harvested at day 3, snap frozen in liquid nitrogen and stored at −80 °C. Protein was isolated from wounds using RIPA buffer (Sigma–Aldrich), and angiogenic cytokine protein levels were quantified using the Mouse Angiogenesis Array Kit (R&D Systems). Pixel density of each spot in the array was quantified using ImageJ.

2.14. Statistical analysis

All values are expressed as mean ± SEM. Statistical significance was determined using the student's unpaired *t* test. A p value < 0.05 was considered statistically significant.

3. Results

3.1. Hydrogel biocompatibility

To assess the feasibility of our previously developed collagen-pullulan hydrogel system as a delivery vehicle for MSCs, we evaluated cell morphology, viability, proliferation and migratory capacity of MSCs cultured within the hydrogels *in vitro*. MSCs attached to pullulan–collagen hydrogels and conformed to the scaffold's three-dimensional topography (Fig. 1A). The majority of cells exhibited a rounded morphology and clustered around the hydrogel pores. MSCs seeded within the hydrogels remained greater than 94% viable for up to two weeks *in vitro* (Fig. 1B). The capacity of MSCs seeded statically on top of hydrogel scaffolds to migrate through the hydrogel matrix was assessed using a transwell migration assay. Twenty-four hours after MSC seeding, a large number of GFP + MSCs were visualized on the permeable membrane separating the two chambers of the transwell support, indicating that MSCs are capable of migrating through the hydrogel (Fig. 1C).

Proliferation of MSCs seeded within the pullulan–collagen hydrogel was compared to MSCs grown in standard two-dimensional cell culture (Fig. 1D). While MSCs cultured on tissue culture plastic demonstrated a normal steady increase in metabolic activity associated with cellular proliferation, MSCs seeded with hydrogel scaffolds showed minimal proliferation over a period of seven days. Given that there was no significant cytotoxicity observed with hydrogel culture conditions, these data suggest that the hydrogel induces MSC quiescence and thus may act as a functional niche for this stem cell population.

3.2. Effect of hydrogel culture on MSC stemness and cytokine secretion

To further investigate changes in the stem cell characteristics of MSCs seeded within three-dimensional hydrogel microenvironments versus MSCs plated onto a standard two-dimensional cell culture dish, we performed real-time PCR analysis of MSCs in their respective *in vitro* conditions (Fig. 2A). MSCs cultured within hydrogels exhibited a significant increase in the relative expression of transcription factors associated with self-renewal and pluripotency including *Oct4* (4.95 ± 0.89, $p = 0.01$), *Sox2* (2.00 ± 0.30, $p < 0.05$), and *Klf4* (1.47 ± 0.21, $p = 0.04$) compared to MSCs in standard cell culture. Western blotting and immunofluorescence staining confirmed the increase in protein levels of these stemness-related transcription factors in MSCs cultured within the hydrogel compared to those plated under standard two-dimensional conditions (Fig. 2B–D).

The gene expression of key wound healing cytokines by MSCs within the hydrogel was also evaluated (Fig. 3). Vascular endothelial growth factor-A (*Vegf-a*) gene expression was significantly induced by culture within the hydrogel (9.82 ± 4.10, $p < 0.05$, Fig. 3A). Similarly, increased relative expression of monocyte chemoattractant protein-1 (*Mcp-1*, 7.72 ± 2.58, $p = 0.02$) was seen in MSCs seeded within a hydrogel compared to those cultured under standard conditions. There was no significant difference in the gene expression of *Fgf-1*, *Sdf-1*, *Angpt2*, *Hgf*, *Angpt1*, *Igf-1* or *Fgf-2* in MSCs grown in either hydrogel or standard culture conditions. To confirm the transcriptional data, we performed ELISAs on conditioned media from both culture conditions. Significantly increased protein levels of both VEGF-A and MCP-1 were found in conditioned media from MSCs within hydrogels compared to those plated in standard conditions ($p < 0.05$, Fig. 3B, C). The augmentation of MSC pluripotency-related transcriptional profile and angiogenic cytokine secretion suggests that use of this hydrogel scaffold for MSC delivery may be an effective strategy to enhance MSC-mediated wound regeneration.

3.3. MSC-seeded scaffold treatment of wild-type murine wounds

To assess the therapeutic efficacy of these MSC-hydrogel constructs in vivo, we utilized a murine model of normal wound healing. Wounds healed significantly faster when treated with MSC-seeded scaffolds compared to local injection of MSCs or no treatment (Fig. 4A, B). Wounds treated with an unseeded hydrogel scaffold alone showed improved early healing but no difference in time to wound closure as we previously reported (data not shown) [22]. There was a significant acceleration of wound healing at day five in both the local MSC injection (56.8 ± 3.2% original wound area, $p = 0.03$) and the MSC-seeded scaffold (50.7 ± 3.3%, $p = 0.002$) groups compared to untreated wounds (69.2 ± 4.3%). However, this early difference in the MSC injection group did not lead to significant differences in time to complete wound closure when compared to untreated wounds. Wounds treated with MSC-seeded scaffolds continued to show significantly improved healing at all time points compared to other treatment groups. MSC-seeded scaffold-treated wounds healed nearly two days faster compared to no treatment in normal (i.e. non-diabetic) animals (day 10.2 ± 0.3 vs. 12.0 ± 0.5, $p = 0.003$). In addition to accelerated wound closure, MSC-seeded scaffold-treated wounds demonstrated more regenerative-like healing with improved skin architecture including a greater return of hair follicles and sebaceous glands (Fig. 4C).

3.4. Assessment of MSC viability and engraftment in vivo

To determine whether the improvements in wound closure were mediated by enhanced MSC viability, we performed bioluminescence imaging on wounds treated with MSCs expressing luciferase (Fig. 5A, B). At 1 h post-wounding, we already observed a decrease in MSC viability following local injection compared to those that were delivered within a hydrogel scaffold (total flux $7.9 \times 10^5 \pm 1.7 \times 10^5$ vs. $1.9 \times 10^6 \pm 5.2 \times 10^5$, $p = 0.06$). The total bioluminescence within the wound was significantly higher in the scaffold-delivery group compared to the injection group at all days examined through day 28 ($p < 0.05$). These data suggest that MSC delivery via a hydrogel scaffold is superior to local injection strategies for maintaining stem cell survival in wounds.

To further investigate MSC engraftment, wound sections were analyzed using immunofluorescence to localize GFP + MSCs within healed wounds at day 14 post-wounding. Fewer GFP + cells were found in wounds treated with injected cells compared to MSC-seeded hydrogel-treated wounds (Fig. 5C). GFP + MSCs in both treatment groups were localized predominantly to the deep dermis surrounding blood vessels and hair follicles. Flow cytometry of wound lysates at days 7 and 14 post-wounding corroborated the histological analyses demonstrating a significantly higher percentage of GFP + cell engraftment with hydrogel delivery compared to local injection (Fig. 5D, day 7, 8.47 ± 1.35% GFP + cells vs. 2.86 ± 1.07%, $p = 0.008$; day 14, 5.63 ± 0.88% vs. 0.57 ± 0.33%, $p = 0.0002$). By day 28 post-wounding, the percentage of GFP + cells within the wounds in both groups decreased further and was no longer significantly different based on flow cytometric analysis (0.46 ± 1.14% MSC-seeded scaffold vs. 0.29 ± 0.94% local MSC injection, $p = 0.90$).

3.5. MSC differentiation in vivo

Having established that MSCs engraft within the wounds, co-localization of GFP with various cell-specific markers was performed on healed wounds at day 14 post-wounding to assess MSC differentiation in vivo (Fig. 6). Using Hsp47 as a fibroblast marker [28], 40.7 ± 11.0% of GFP + cells delivered into wounds via a hydrogel scaffold appeared to have differentiated into dermal fibroblasts (Fig. 6A). No GFP + cells were found within the healed epidermis indicating that MSCs delivered within the hydrogel scaffolds had not differentiated into keratinocytes (Fig. 5B). Co-staining for GFP and the pericyte marker NG2 [29] demonstrated that 38.7 ± 8.0% of MSCs had differentiated into pericytes (Fig. 6C). A smaller percentage (12.5 ± 4.6%) of GFP + MSCs were found to coexpress the endothelial cell-specific marker CD31 (Fig. 6D). Altogether, more than half of all GFP + cells within healed wounds were associated with the vasculature.

3.6. Wound vascularization

Excisional wounds treated with either injected or hydrogel-delivered MSCs appeared grossly more vascular than untreated wounds (data not shown). To characterize wound vascularization, the number of dermal microvessels were counted in H&E-stained sections of healed day 14 wounds (Fig. 7A, B). There was a moderate increase in the number of microvessels in wounds treated with local injection of MSCs (4.3 ± 0.4 vessels per hpf vs. 2.8 ± 0.5, $p = 0.03$), but neovascularization was further augmented when MSCs were

delivered within the biomimetic scaffold (8.0 ± 0.7 vessels per hpf; vs. untreated $p = 1.2 \times 10^{-7}$; vs. injection $p = 3.0 \times 10^{-5}$). The increase in vascularization seen in MSC-seeded hydrogel-treated wounds was confirmed with CD31 immunofluorescent staining (Fig. 7C, D). There was no significant difference in CD31 staining intensity in wounds treated with local MSC injection compared to untreated wounds (4121 ± 1500 vs. 2211 ± 901 pixels, $p = 0.34$). CD31 staining was significantly increased in wounds treated with MSC-seeded scaffolds compared to untreated wounds (6416 ± 741 vs. 2211 ± 901 pixels, $p = 0.02$).

To assess the role of pro-angiogenic cytokines in the MSC-mediated improvements in vascularization, protein was isolated from wounds at day 3, and cytokine levels were quantified using a mouse angiogenesis array (Fig. 7E, F). We first looked at those angiogenic cytokines whose gene expression was induced by hydrogel culture *in vitro* (Fig. 7E). There was no significant difference in MCP-1 protein levels in untreated wounds compared to wounds treated with local MSC injection (0.60 ± 0.04 vs. 0.52 ± 0.04 relative pixel density compared to positive control, $p = 0.17$). Wounds treated with MSC-seeded hydrogels had significantly higher levels of MCP-1 compared to untreated controls (0.76 ± 0.10 vs. 0.52 ± 0.04, $p = 0.05$), although the difference in MCP-1 protein levels in MSC-seeded hydrogel-treated and local MSC injection-treated wounds was not significant ($p = 0.15$). Local injection of MSCs did not appreciablyalter protein levels of VEGF-A or VEGF-B in wounds (VEGF-A 0.04 ± 0.005 vs. 0.05 ± 0.09, $p = 0.48$; VEGF-B 0.03 ± 0.007 vs. 0.03 ± 0.006, $p = 0.95$). However, wounds treated with MSC-seeded hydrogels demonstrated significantly increased VEGF-A (0.13 ± 0.04, $p = 0.06$ vs. untreated, $p < 0.05$ vs. MSC injection) and VEGF-B (0.09 ± 0.02, $p = 0.03$ vs. untreated and MSC injection) compared to both untreated and local MSC injection-treated wounds.

Several other pro-angiogenic factors were found to be differentially expressed when MSCs were delivered via injection versus hydrogel scaffolds (Fig. 7F). FGF-1 protein levels in MSC-seeded scaffold-treated wounds (0.26 ± 0.01) were significantly higher than those found in untreated (0.17 ± 0.03, $p < 0.05$) and local MSC injection-treated wounds (0.21 ± 0.01, $p = 0.02$). Similarly, the matrix metalloproteinases MMP-8 and MMP-9 were found at significantly higher levels in wounds treated with MSC-seeded scaffolds (MMP-8: 0.62 ± 0.01; MMP-9: 0.91 ± 0.01) compared to untreated (MMP-8: 0.30 ± 0.05, $p = 0.002$; MMP-9: 0.61 ± 0.05, $p = 0.002$) and local MSC injection-treated wounds (MMP-8: 0.34 ± 0.06, $p = 0.004$; MMP-9: 0.76 ± 0.04, $p = 0.007$). These data suggest that the induction of VEGF and other key cytokines by our MSC-seeded hydrogel translates to significantly augmented vascularization through multiple angiogenic pathways.

4. Discussion

In this study, we utilize a biomimetic hydrogel scaffold to effectively deliver MSCs into cutaneous wounds. Our tissue engineering approach to MSC-based wound therapy enhances the stemness properties of these cells as well as their capacity to secrete cytokines critical to healing. Compared to local MSC injection, delivery of MSCs within a pullulan–collagen hydrogel scaffold accelerates wound healing, improves stem cell survival and promotes angiogenesis.

Previous studies have demonstrated the capacity of hydrogel systems to support the self-renewal of embryonic stem cells (ESCs) and to maintain these cells in their undifferentiated state [30,31]. While these synthetic matrices have provided a means of circumventing feeder layers for ESC culture, adult MSCs do not require culture on feeder layers. However, the loss of stem-like properties and spontaneous differentiation of MSCs over time in standard *in vitro* conditions has been described [32], which dilutes the multipotency of the population and may diminish the capacity of these cells to contribute pro-regenerative paracrine factors and to replenish multiple cell types within wounds. Our findings demonstrate that culture of MSCs within a hydrogel system can maintain their stemness properties and thus functions as a synthetic equivalent of the stem cell niche.

The powerful role of MSCs as paracrine effectors has been demonstrated in previous studies [7]. We demonstrate here that the structural microenvironment can significantly alter MSC behavior and can be used to manipulate their cytokine secretion profile. VEGF-A and MCP-1 both contribute significantly to the angiogenic response post-wounding [33,34], and a biomaterial approach to enhance the secretion of these important cytokines would likely be useful in pathologic healing conditions. Further, both VEGF-A and MCP-1 have been implicated in the trafficking of MSCs to sites of injury [35,36], thus potentially enabling delivered exogenous MSCs to effectively recruit endogenous stem cells. While the mechanism responsible for this upregulation of angiogenic cytokines and stemness factors is currently under investigation, it is possible that the hydrogel microenvironment is hypoxic relative to standard culture in ambient conditions. Hypoxic preconditioning has been previously shown to upregulate MSC expression of both *Vegf* [37] and *Oct4* [38] and can enhance MSC survival and regenerative potential in vivo [39]. Future experiments will be aimed at further defining the hydrogel microenvironment and elucidating the mechanisms behind the hydrogel-induced enhancement of MSC regenerative potential.

The impaired survival of stem and progenitor cells injected directly into a site of tissue injury has been demonstrated by our laboratory and others [40,41]. Concordantly in this study, we observed a dramatic decrease in MSC viability as early as 1 h post-injection. This finding suggests that the injection of MSCs into a closed space may be inherently cytotoxic, potentially due to shear forces during injection or the lack of cell–matrix interactions leading to anoikis. In contrast, the use of a hydrogel scaffold for short-term MSC culture and subsequent cell delivery significantly enhances MSC survival within the hostile wound microenvironment. Although MSC viability within the wound gradually diminishes over time in all conditions that we tested in this study, we have shown that the method of MSC delivery can significantly alter the number of cells present throughout wound healing. Our data suggest that enhanced MSC survival and function in the first two to three weeks post-wounding is sufficient to promote accelerated wound healing and that long-term engraftment of cells may not be necessary.

The augmentation of MSC viability through delivery within a hydrogel scaffold is in turn associated with the improved functional outcomes of increased vascularization and enhanced wound healing. Although previous studies have demonstrated improvements in wound healing using injection methods to deliver MSCs into wounds [1,2,5], we did not appreciate a significant difference in healing using this methodology. These prior studies

used four to eight times as many MSCs as our injection studies, but we were unable to use this high number of cells due to the logistics of cell seeding onto a small hydrogel scaffold. We postulate that this increased therapeutic dose may account for the differences in wound healing noted by other groups. Further while it is not evident from these experiments whether this improvement in wound healing is due merely to an increased number of viable MSCs or to their enhanced regenerative potential induced by short-term culture within the hydrogel, this continues to be an area of ongoing investigation in our laboratory.

The use of a tissue-engineered scaffold as a delivery vehicle for stem and progenitor cells has proven beneficial for enhancement of cell engraftment in previous studies of injury models in the heart [14] and ischemic hindlimb [41]. However, while other groups have developed various cell delivery systems to implant stem cells into wounds [20,42], we demononstate here the therapeutic superiority of a tissue-engineered construct for delivery of stem cells into cutaneous wounds compared to direct injection methods. We have demonstrated that by delivering MSCs within a biomimetic hydrogel scaffold we can significantly augment the number of MSCs present in the wound environment throughout the repair process. At day 28 post-wounding, the number of engrafted MSCs delivered via the hydrogel did not appear significantly different than the number of engrafted MSCs delivered via local injection. However, as all wounds had closed by day 14, the enhancement of MSC engraftment efficiency at earlier time points during the inflammation and proliferation stages of wound healing is likely more important to the functional endpoints of wound closure and vascularization.

The differentiation of transplanted MSCs into keratinocytes, endothelial cells, sebocytes and pericytes within cutaneous wounds has been reported by several groups [2,43,44]. However, whether the fate of MSCs within wounds can be regulated by microenvironmental cues within the delivery vehicle has not been previously investigated. While we did see significantly different numbers of engrafted cells with different delivery methods, the fate of transplanted MSCs did not appear to change significantly between local injection or hydrogel delivery. It is possible that while survival of MSCs is promoted through the maintainence of cell–matrix interactions and other protective factors provided by the hydrogel, the control of stem cell fate determination may require more complex structural and biochemical cues to be incorporated within the hydrogel design. Further, the scope of the cell-specific markers that we investigated with immunofluorescent staining was not broad enough to determine the ultimate fate of all GFP + MSCs delivered within our hydrogel scaffold. There remained 8.1% of GFP + cells in the MSC-seeded scaffold-treated wounds that we were unable to identify with our cell surface marker panel. This unidentified population could potentially have included sebocytes, dendritic cells, or various inflammatory cells. Given our *in vitro* data demonstrating that MSCs within the hydrogel express increased levels of stemness genes, it is possible that MSCs within our hydrogel scaffold may have enhanced plasticity to contribute to non-mesenchymal cell populations within healing cutaneous wounds.

We provide evidence here that normal, unimpaired healing can be accelerated through the use of an MSC-hydrogel construct. Treatment with this MSC-seeded scaffold augmented the angiogenic response in these normal animals and was associated with an early upregulation

of angiogenic cytokines. Although we did not evaluate the use of our MSC-seeded hydrogel in models of pathologic healing such as that seen in diabetes, these results lead us to expect an even greater therapeutic response in situations where the angiogenic response is impaired.

5. Conclusion

These findings demonstrate the capacity of a biomimetic hydrogel system to enhance MSC delivery to cutaneous wounds potentially by preserving cell–matrix interactions, localizing cells within wounds and enhancing stem cell properties. Hydrogel delivery of MSCs significantly enhances MSC viability and engraftment compared to local injection. Biomimetic hydrogels provide a functionalized niche for the in vivo delivery of MSCs which accelerates normal wound healing and promotes neovascularization. Further modifications of the hydrogel matrix to enhance its niche-like characteristics may provide further regenerative benefits to this MSC-based therapeutic construct.

Acknowledgments

This work was supported by a grant to GCG and MTL from the Armed Forces Institute of Regenerative Medicine DOD #W81XWH-08-2-0032, the Hagey Laboratory for Pediatric Regenerative Medicine and the Oak Foundation. We gratefully acknowledge Mrs. Yujin Park for histologic processing, and Mr. Dean Nehama and Ms. Jessica Trang of the Stanford BioADD Center for assistance with hydrogel preparation.

References

1. Wu Y, Chen L, Scott PG, Tredget EE. Mesenchymal stem cells enhance wound healing through differentiation and angiogenesis. Stem Cells. 2007; 25(10):2648–59. [PubMed: 17615264]
2. Sasaki M, Abe R, Fujita Y, Ando S, Inokuma D, Shimizu H. Mesenchymal stem cells are recruited into wounded skin and contribute to wound repair by transdifferentiation into multiple skin cell type. J Immunol. 2008; 180(4):2581–7. [PubMed: 18250469]
3. Satoh H, Kishi K, Tanaka T, Kubota Y, Nakajima T, Akasaka Y, et al. Transplanted mesenchymal stem cells are effective for skin regeneration in acute cutaneous wounds. Cell Transplant. 2004; 13(4):405–12. [PubMed: 15468682]
4. Deng W, Han Q, Liao L, Li C, Ge W, Zhao Z, et al. Engrafted bone marrow-derived flk-(1þ) mesenchymal stem cells regenerate skin tissue. Tissue Eng. 2005; 11(1–2):110–9. [PubMed: 15738666]
5. Fu X, Fang L, Li X, Cheng B, Sheng Z. Enhanced wound-healing quality with bone marrow mesenchymal stem cells autografting after skin injury. Wound Repair Regen. 2006; 14(3):325–35. [PubMed: 16808812]
6. Liu P, Deng Z, Han S, Liu T, Wen N, Lu W, et al. Tissue-engineered skin containing mesenchymal stem cells improves burn wounds. Artif Organs. 2008; 32(12):925–31. [PubMed: 19133020]
7. Chen L, Tredget EE, Wu PY, Wu Y. Paracrine factors of mesenchymal stem cells recruit macrophages and endothelial lineage cells and enhance wound healing. PLoS One. 2008; 3(4):e1886. [PubMed: 18382669]
8. Hocking AM, Gibran NS. Mesenchymal stem cells: paracrine signaling and differentiation during cutaneous wound repair. Exp Cell Res. 2010; 316(14):2213–9. [PubMed: 20471978]
9. Wagner J, Kean T, Young R, Dennis JE, Caplan AI. Optimizing mesenchymal stem cell-based therapeutics. Curr Opin Biotechnol. 2009; 20(5):531–6. [PubMed: 19783424]
10. Lee RH, Seo MJ, Reger RL, Spees JL, Pulin AA, Olson SD, et al. Multipotent stromal cells from human marrow home to and promote repair of pancreatic islets and renal glomeruli in diabetic NOD/scid mice. Proc Natl Acad Sci U S A. 2006; 103(46):17438–43. [PubMed: 17088535]

11. Iso Y, Spees JL, Serrano C, Bakondi B, Pochampally R, Song YH, et al. Multipotent human stromal cells improve cardiac function after myocardial infarction in mice without long-term engraftment. Biochem Biophys Res Commun. 2007; 354(3):700–6. [PubMed: 17257581]
12. Burst VR, Gillis M, Putsch F, Herzog R, Fischer JH, Heid P, et al. Poor cell survival limits the beneficial impact of mesenchymal stem cell transplantation on acute kidney injury. Nephron Exp Nephrol. 2010; 114(3):e107–16. [PubMed: 19955830]
13. di Bonzo LV, Ferrero I, Cravanzola C, Mareschi K, Rustichell D, Novo E, et al. Human mesenchymal stem cells as a two-edged sword in hepatic regenerative medicine: engraftment and hepatocyte differentiation versus profibrogenic potential. Gut. 2008; 57(2):223–31. [PubMed: 17639088]
14. Simpson D, Liu H, Fan TH, Nerem R, Dudley SC Jr. A tissue engineering approach to progenitor cell delivery results in significant cell engraftment and improved myocardial remodeling. Stem Cells. 2007; 25(9):2350–7. [PubMed: 17525236]
15. Kutschka I, Chen IY, Kofidis T, Arai T, von Degenfeld G, Sheikh AY, et al. Collagen matrices enhance survival of transplanted cardiomyoblasts and contribute to functional improvement of ischemic rat hearts. Circulation. 2006; 114(1 Suppl):I167–73. [PubMed: 16820568]
16. Suuronen EJ, Veinot JP, Wong S, Kapila V, Price J, Griffith M, et al. Tissueengineered injectable collagen-based matrices for improved cell delivery and vascularization of ischemic tissue using CD133þ progenitors expanded from the peripheral blood. Circulation. 2006; 114(1 Suppl):I138–44. [PubMed: 16820563]
17. Lund AW, Yener B, Stegemann JP, Plopper GE. The natural and engineered 3D microenvironment as a regulatory cue during stem cell fate determination. Tissue Eng Part B Rev. 2009; 15(3):371–80. [PubMed: 19505193]
18. Gurtner GC, Werner S, Barrandon Y, Longaker MT. Wound repair and regeneration. Nature. 2008; 453(7193):314–21. [PubMed: 18480812]
19. Mooney DJ, Vandenburgh H. Cell delivery mechanisms for tissue repair. Cell Stem Cell. 2008; 2(3):205–13. [PubMed: 18371446]
20. Altman AM, Matthias N, Yan Y, Song YH, Bai X, Chiu ES, et al. Dermal matrix as a carrier for in vivo delivery of human adipose-derived stem cells. Biomaterials. 2008; 29(10):1431–42. [PubMed: 18191190]
21. Lutolf MP, Hubbell JA. Synthetic biomaterials as instructive extracellular microenvironments for morphogenesis in tissue engineering. Nat Biotechnol. 2005; 23(1):47–55. [PubMed: 15637621]
22. Wong VW, Rustad KC, Galvez MG, Neofyotou E, Glotzbach JP, Januszyk M, et al. Engineered pullulan-collagen composite dermal hydrogels improve early cutaneous wound healing. Tissue Eng Part A. 2011; 17(5–6):631–44. [PubMed: 20919949]
23. Hamou C, Callaghan MJ, Thangarajah H, Chang E, Chang EI, Grogan RH, et al. Mesenchymal stem cells can participate in ischemic neovascularization. Plast Reconstr Surg. 2009; 123(2 Suppl): 45S–55S. [PubMed: 19182663]
24. Yang HN, Park JS, Na K, Woo DG, Kwon YD, Park KH. The use of green fluorescence gene (GFP)-modified rabbit mesenchmal stem cells (rMSCs) cocultured with chondrocytes in hydrogel constructs to reveal the chondrogenesis of MSCs. Biomaterials. 2009; 30(31):6374–85. [PubMed: 19682739]
25. Wang C, Hao J, Zhang F, Su K, Wang DA. RNA extraction from polysaccharidebased cell-laden hydrogel scaffolds. Anal Biochem. 2008; 380(2):333–4. [PubMed: 18582431]
26. Galiano RD, Michaels Jt, Dobryansky M, Levine JP, Gurtner GC. Quantitative and reproducible murine model of excisional wound healing. Wound Repair Regen. 2004; 12(4):485–92. [PubMed: 15260814]
27. Marlow R, Binnewies M, Sorensen LK, Monica SD, Strickland P, Forsberg EC, et al. Vascular Robo4 restricts proangiogenic VEGF signaling in breast. Proc Natl Acad Sci U S A. 2010; 107(23):10520–5. [PubMed: 20498081]
28. Kuroda K, Tajima S. HSP47 is a useful marker for skin fibroblasts in formalin-fixed, paraffin-embedded tissue specimens. J Cutan Pathol. 2004; 31(3):241–6. [PubMed: 14984576]

29. Ozerdem U, Grako KA, Dahlin-Huppe K, Monosov E, Stallcup WB. NG2 proteoglycan is expressed exclusively by mural cells during vascular morphogenesis. Dev Dyn. 2001; 222(2):218–27. [PubMed: 11668599]
30. Gerecht S, Burdick JA, Ferreira LS, Townsend SA, Langer R, Vunjak-Novakovic G. Hyaluronic acid hydrogel for controlled self-renewal and differentiation of human embryonic stem cells. Proc Natl Acad Sci U S A. 2007; 104(27):11298–303. [PubMed: 17581871]
31. Li YJ, Chung EH, Rodriguez RT, Firpo MT, Healy KE. Hydrogels as artificial matrices for human embryonic stem cell self-renewal. J Biomed Mater Res A. 2006; 79(1):1–5. [PubMed: 16741988]
32. Tsai CC, Chen CL, Liu HC, Lee YT, Wang HW, Hou LT, et al. Overexpression of hTERT increases stem-like properties and decreases spontaneous differentiation in human mesenchymal stem cell lines. J Biomed Sci. 2010; 17:64. [PubMed: 20670406]
33. Yancopoulos GD, Davis S, Gale NW, Rudge JS, Wiegand SJ, Holash J. Vascularspecific growth factors and blood vessel formation. Nature. 2000; 407(6801):242–8. [PubMed: 11001067]
34. Ma J, Wang Q, Fei T, Han JD, Chen YG. MCP-1 mediates TGF-beta-induced angiogenesis by stimulating vascular smooth muscle cell migration. Blood. 2007; 109(3):987–94. [PubMed: 17032917]
35. Tang JM, Wang JN, Zhang L, Zheng F, Yang JY, Kong X, et al. VEGF/SDF-1 promotes cardiac stem cell mobilization and myocardial repair in the infarcted heart. Cardiovasc Res. 2011; 91(3): 402–11. [PubMed: 21345805]
36. Belema-Bedada F, Uchida S, Martire A, Kostin S, Braun T. Efficient homing of multipotent adult mesenchymal stem cells depends on FROUNT-mediated clustering of CCR2. Cell Stem Cell. 2008; 2(6):566–75. [PubMed: 18522849]
37. Annabi B, Lee YT, Turcotte S, Naud E, Desrosiers RR, Champagne M, et al. Hypoxia promotes murine bone-marrow-derived stromal cell migration and tube formation. Stem Cells. 2003; 21(3): 337–47. [PubMed: 12743328]
38. Grayson WL, Zhao F, Bunnell B, Ma T. Hypoxia enhances proliferation and tissue formation of human mesenchymal stem cells. Biochem Biophys Res Commun. 2007; 358(3):948–53. [PubMed: 17521616]
39. Rosova I, Dao M, Capoccia B, Link D, Nolta JA. Hypoxic preconditioning results in increased motility and improved therapeutic potential of human mesenchymal stem cells. Stem Cells. 2008; 26(8):2173–82. [PubMed: 18511601]
40. Chang EI, Bonillas RG, El-ftesi S, Chang EI, Ceradini DJ, Vial IN, et al. Tissue engineering using autologous microcirculatory beds as vascularized bioscaffolds. FASEB J. 2009; 23(3):906–15. [PubMed: 19001054]
41. Silva EA, Kim ES, Kong HJ, Mooney DJ. Material-based deployment enhances efficacy of endothelial progenitor cells. Proc Natl Acad Sci U S A. 2008; 105(38):14347–52. [PubMed: 18794520]
42. Falanga V, Iwamoto S, Chartier M, Yufit T, Butmarc J, Kouttab N, et al. Autologous bone marrow-derived cultured mesenchymal stem cells delivered in a fibrin spray accelerate healing in murine and human cutaneous wounds. Tissue Eng. 2007; 13(6):1299–312. [PubMed: 17518741]
43. Badiavas EV, Abedi M, Butmarc J, Falanga V, Quesenberry P. Participation of bone marrow derived cells in cutaneous wound healing. J Cell Physiol. 2003; 196(2):245–50. [PubMed: 12811816]
44. Kataoka K, Medina RJ, Kageyama T, Miyazaki M, Yoshino T, Makino T, et al. Participation of adult mouse bone marrow cells in reconstitution of skin. Am J Pathol. 2003; 163(4):1227–31. [PubMed: 14507632]

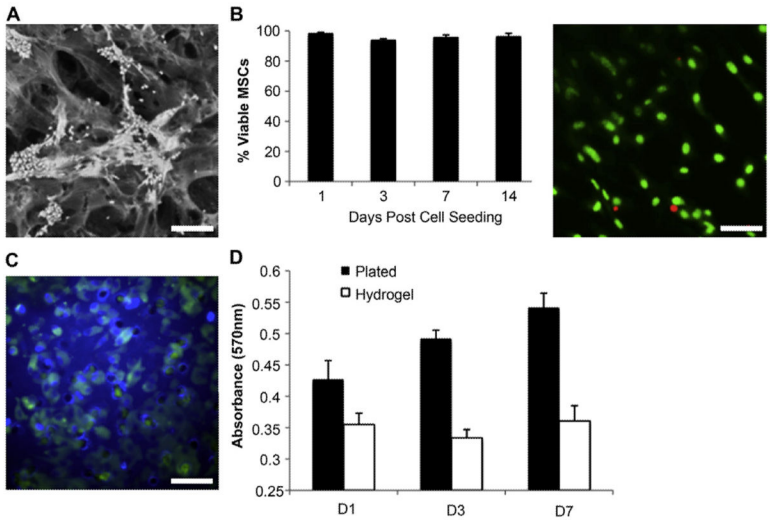

Fig. 1.

Biocompatibility of murine MSCs within a biomimetic pullulan–collagen hydrogel. (A) Scanning micrograph of MSCs seeded in a hydrogel scaffold for 24 h. Scale bar 100 μm. (B) Live/dead assay of MSCs seeded within hydrogel *in vitro*. Right panel is representative image at 14 days. Scale bar 40 μm. (C) Transwell migration assay demonstrates migratory capacity of MSCs through the hydrogel. Scale bar 40 μm. (D) An MTT assay was used to assess MSC proliferation over seven days.

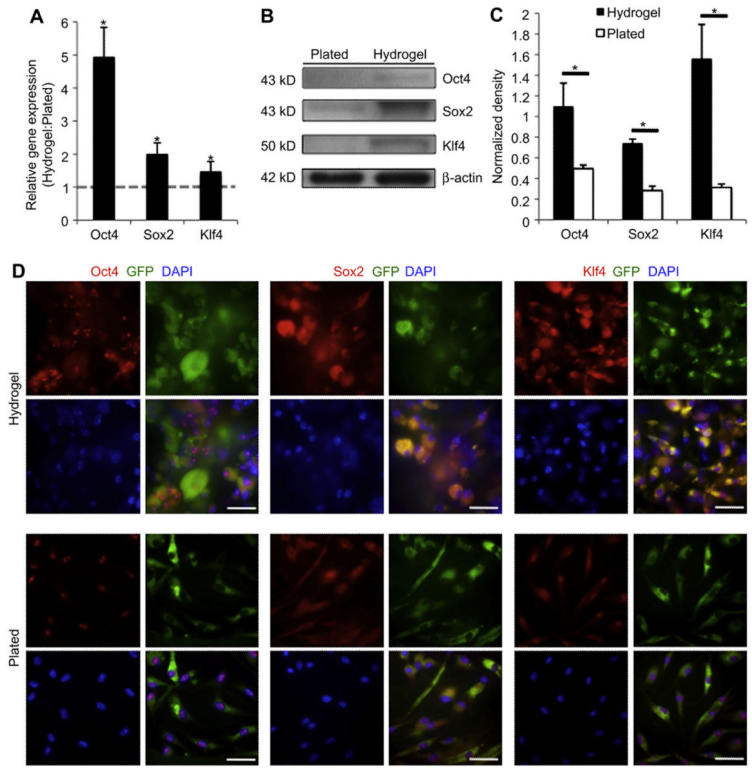

Fig. 2.

MSC expression of stemness genes. (A): qRT-PCR analysis of *Oct4*, *Sox2* and *Klf4* gene expression in hydrogel culture versus standard plating (dotted grey line, $n = 7$). (B): Western blotting of stemness genes. (C) Quantification of western blotting ($n = 4$). (D): Immunofluorescent staining demonstrates that MSCs cultured within the hydrogel express increased levels of stem cell-related genes. Scale bar 40 μm $^{*}p < 0.05$.

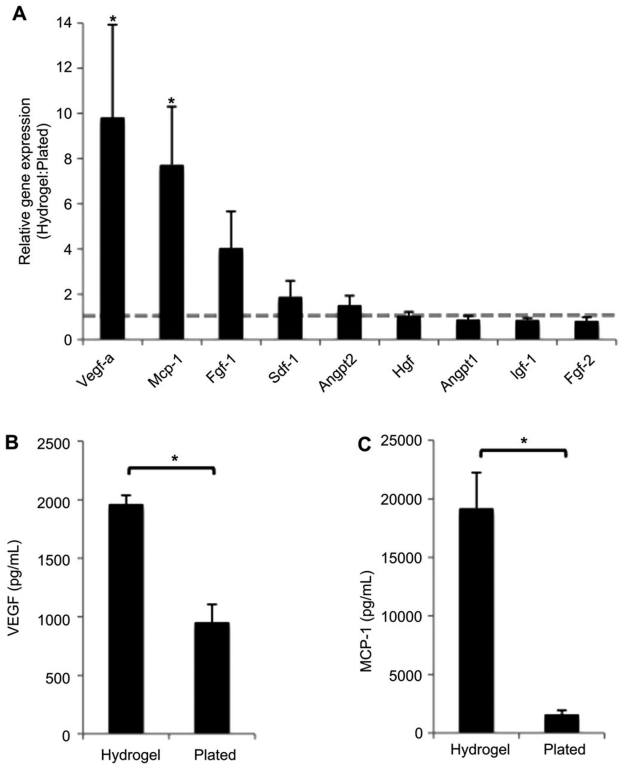

Fig. 3.

MSC cytokine secretion. (A): qRT-PCR analysis of key wound healing cytokines known to be secreted by MSCs (dotted grey line indicates baseline expression of plated MSCs, $n = 7$). (B): Protein levels of VEGF-A and (C): MCP-1 in conditioned media from MSCs cultured in hydrogels compared to those plated under standard conditions ($n = 8$). *$p < 0.05$.

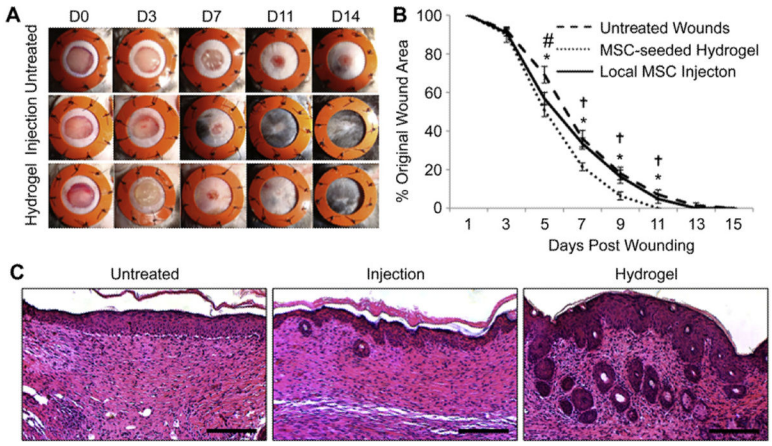

Fig. 4.

Effects of MSC delivery method on wound closure. (A): Gross photos. (B): Wound closure curves demonstrate significantly accelerated healing in wounds treated with MSC-seeded hydrogels. (C): H&E staining of wounds at day 14. Scale bar 100 μm *$p < 0.05$ untreated vs. MSC-seeded scaffold, #$p < 0.05$ untreated vs. local MSC injection, †$p < 0.05$ local MSC injection vs. MSC-seeded scaffold.

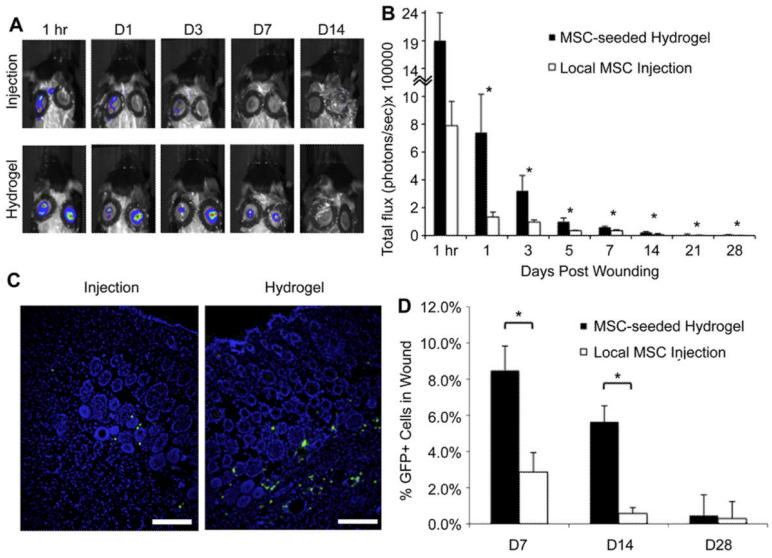

Fig. 5.

In vivo MSC viability and engraftment. (A): Bioluminescence imaging was used to follow luciferase + MSCs delivered into wounds. (B): Quantification of total flux. (C): Immunofluorescent images of GFP + MSCs within day 14 wounds. Scale bar 100 μm (D): Flow cytometric quantification of GFP + cells in wounds. *$p < 0.05$.

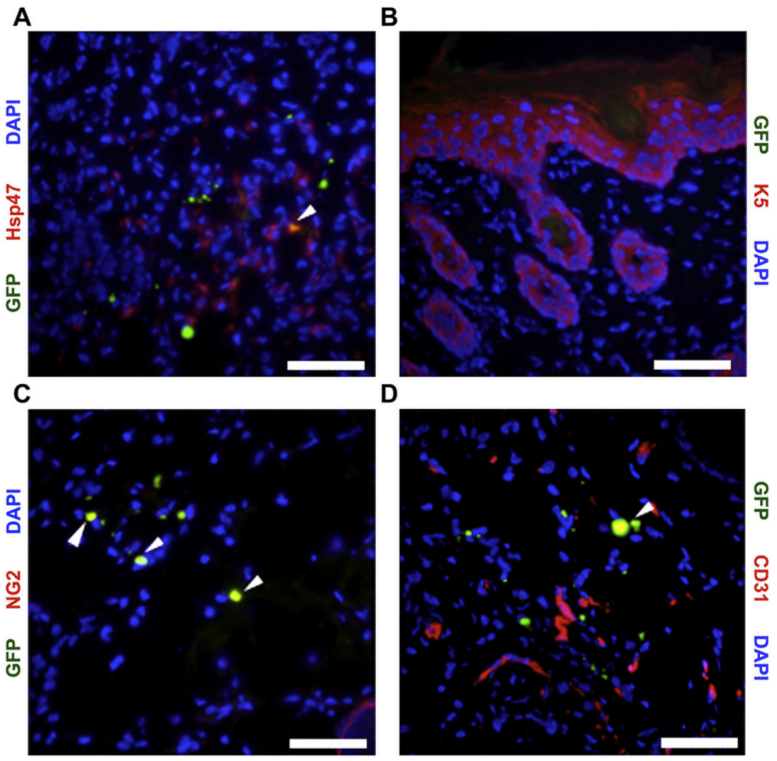

Fig. 6.

Co-localization of GFP + MSCs with cell-specific markers to determine MSC fate within wounds. MSCs co-localized (yellow, arrowheads) with Hsp47 (A), NG2 (C), and CD31 (D). (B): No GFP+/K5+ cells were observed. Scale bar 20 μm. (For interpretation of the references to colour in this figure legend, the reader is referred to the web version of this article.)

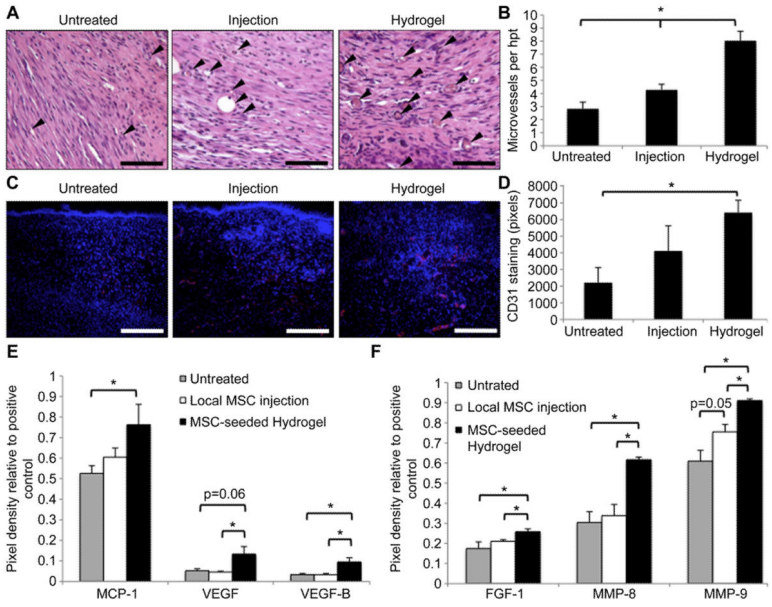

Fig. 7.

Effect of MSC delivery method on wound vascularization. (A): H&E-stained sections of day 14 wounds. Arrowheads indicate microvessels. Scale bar 20 μm (B): Microvessel counts. (C): Day 14 wounds stained for CD31 (red). Scale bar 100 μm (D): Quantification of CD31 staining intensity. (E,F): Evaluation of wound angiogenic cytokine levels at day 3 post-wounding. *$p <$ 0.05. (For interpretation of the references to colour in this figure legend, the reader is referred to the web version of this article.)